AMERICAN SOCIETY FOR MICROBIOLOGY | Applied and Environmental Microbiology®

PUBLIC AND ENVIRONMENTAL HEALTH MICROBIOLOGY

Relative Abundances of *Candida albicans* and *Candida glabrata* in *In Vitro* Coculture Biofilms Impact Biofilm Structure and Formation

Michelle L. Olson,[a] Arul Jayaraman,[a] Katy C. Kao[a]

[a]Department of Chemical Engineering, Texas A&M University, College Station, Texas, USA

ABSTRACT *Candida* is a member of the normal human microbiota and often resides on mucosal surfaces such as the oral cavity or the gastrointestinal tract. In addition to their commensality, *Candida* species can opportunistically become pathogenic if the host microbiota is disrupted or if the host immune system becomes compromised. An important factor for *Candida* pathogenesis is its ability to form biofilm communities. The two most medically important species—*Candida albicans* and *Candida glabrata*—are often coisolated from infection sites, suggesting the importance of *Candida* coculture biofilms. In this work, we report that biofilm formation of the coculture population depends on the relative ratio of starting cell concentrations of *C. albicans* and *C. glabrata*. When using a starting ratio of *C. albicans* to *C. glabrata* of 1:3, ~6.5- and ~2.5-fold increases in biofilm biomass were observed relative to those of a *C. albicans* monoculture and a *C. albicans*/*C. glabrata* ratio of 1:1, respectively. Confocal microscopy analysis revealed the heterogeneity and complex structures composed of long *C. albicans* hyphae and *C. glabrata* cell clusters in the coculture biofilms, and reverse transcription-quantitative PCR (qRT-PCR) studies showed increases in the relative expression of the *HWP1* and *ALS3* adhesion genes in the *C. albicans*/*C. glabrata* 1:3 biofilm compared to that in the *C. albicans* monoculture biofilm. Additionally, only the 1:3 *C. albicans*/*C. glabrata* biofilm demonstrated an increased resistance to the antifungal drug caspofungin. Overall, the results suggest that interspecific interactions between these two fungal pathogens increase biofilm formation and virulence-related gene expression in a coculture composition-dependent manner.

IMPORTANCE *Candida albicans* and *Candida glabrata* are often coisolated during infection, and the occurrence of coisolation increases with increasing inflammation, suggesting possible synergistic interactions between the two *Candida* species in pathogenesis. During the course of an infection, the prevalence of each *Candida* species may change over time due to differences in metabolism and in the resistance of each species to antifungal therapies. Therefore, it is necessary to understand the dynamics between *C. albicans* and *C. glabrata* in coculture to develop better therapeutic strategies against *Candida* infections. Existing *in vitro* work has focused on understanding how an equal-part culture of *C. albicans* and *C. glabrata* impacts biofilm formation and pathogenesis. What is not understood, and what is investigated in this work, is how the composition of *Candida* species in coculture impacts overall biofilm formation, virulence gene expression, and the therapeutic treatment of biofilms.

KEYWORDS *Candida*, biofilm, coculture, CLSM, mycobiota, biofilms

The human microbiota is composed of a diverse array of bacterial and fungal species that colonize different sites in the body (1, 2). Although the composition and function of the bacteria in the microbiota have been extensively studied (3–7), the mycobiota, or fungal members of the microbiome, remains largely understudied (1). In

Received 14 December 2017 **Accepted** 26 January 2018

Accepted manuscript posted online 2 February 2018

Citation Olson ML, Jayaraman A, Kao KC. 2018. Relative abundances of *Candida albicans* and *Candida glabrata* in *in vitro* coculture biofilms impact biofilm structure and formation. Appl Environ Microbiol 84:e02769-17. https://doi.org/10.1128/AEM.02769-17.

Editor Andrew J. McBain, University of Manchester

Address correspondence to Arul Jayaraman, arulj@mail.che.tamu.edu, or Katy C. Kao, kao.katy@tamu.edu.

the gastrointestinal tract, shotgun sequencing revealed that fungi comprise approximately 0.1% of the microorganisms (8, 9), yet this is likely an underrepresentation (1). Some of the most common fungi in the human body are *Candida* spp., which colonize mucosal surfaces such as the oral cavity, gastrointestinal (GI) tract, urogenital tract, and also the skin in approximately 70% of healthy individuals (10). An expansion in the *Candida* population may lead to mucosal and deep tissue infections (candidiasis), while disseminated candidiasis (candidemia) often affects patients on broad-spectrum antibiotics or antifungal drugs, patients with chronic inflammation, nosocomial patients, and patients that are immunocompromised, such as those with HIV or AIDS (11, 12). Not surprisingly, *Candida* is the fourth leading cause of nosocomial infections, and candidemia mortality rates may be as high as 50% (13–15).

Of the various *Candida* spp., the opportunistic pathogens *Candida albicans* and *Candida glabrata* account for roughly 60% of *Candida* spp. in the human body. *C. albicans* is often the leading cause of candidiasis and candidemia, with *C. glabrata* frequently reported as the second most common *Candida* isolate in infections within North America (13, 16–18). *C. albicans* and *C. glabrata* are often coisolated together during an infection, and the isolation of a single species, *C. glabrata*, from infection sites is rare (19). Additionally, the coisolation of *C. albicans* and *C. glabrata* has been linked to increased pathogenesis, as the occurrence of coisolation was reported in almost 80% of patients with severe inflammation (20). The inherent resistance of *C. glabrata* against commonly used antifungals such as fluconazole and amphotericin B is generally higher than that of *C. albicans* (21, 22). The abundances of *C. glabrata* and non-*albicans* *Candida* species have been shown to increase in a clinical study during a course of antifungal treatment against *Candida* spp. (13). Nguyen et al. (16) observed 427 nosocomial patients with candidemia and found that after treatment with amphotericin B, *C. glabrata* was the most common non-*albicans* *Candida* species to cause candidemia, mainly due to the persistence of *C. glabrata* and its resistance to antifungal treatment (16).

Biofilm communities provide a protective niche for microorganisms from stress and external perturbations, and it is estimated that 65% to 80% of human infections originate from biofilms (23). Fungal species such as *Candida* are also found in polymicrobial biofilms in the human body and are generally more resistant to antifungal agents than when present in suspension (24). It has also been shown that the biofilm microenvironment facilitates *Candida* in evading the host immune system and persisting in the body (25, 26). *Candida albicans* not only resides in the biofilm but also contributes to its development, as it is also capable of forming robust biofilms (27, 28). This is primarily due to its polymorphic nature, as it is able to grow as yeast, pseudohyphae, and hyphae. The hyphal morphology of *C. albicans* is associated with an increased virulence, as it enables the active penetration of mucosal surfaces into host tissue, which can lead to disseminated candidiasis. On the other hand, *C. glabrata* mainly grows as a budding yeast and has been shown to attach to hyphae of *C. albicans* to invade tissue (29). The presence of *Candida* spp. in a polymicrobial biofilm not only promotes its virulence but also increases the biofilm formation and antimicrobial resistance of other pathogenic bacteria, as has been demonstrated for *Staphylococcus aureus* (30).

Despite the synergism between *C. albicans* and *C. glabrata*, there is limited information on the underlying mechanisms involved in the interaction between the two fungal species and their effects on virulence and invasion. Recent work by Pathak et al. with *C. albicans* and *C. glabrata* cocultures demonstrated that cocultures with a 1:1 initial ratio of *C. albicans* to *C. glabrata* yielded the highest biofilm biomass over any other *Candida* species combination as well as over single-species biofilms (31). In addition, a recent host microbiome study showed that the abundances of fungal species, including *C. albicans*, changed with diet and potentially contributed to disease (32); thus, it is conceivable that the relative abundance of a fungal species within a polymicrobial biofilm can impact pathogenesis. However, there is little knowledge regarding the relative abundance of each species in a biofilm and how that contributes

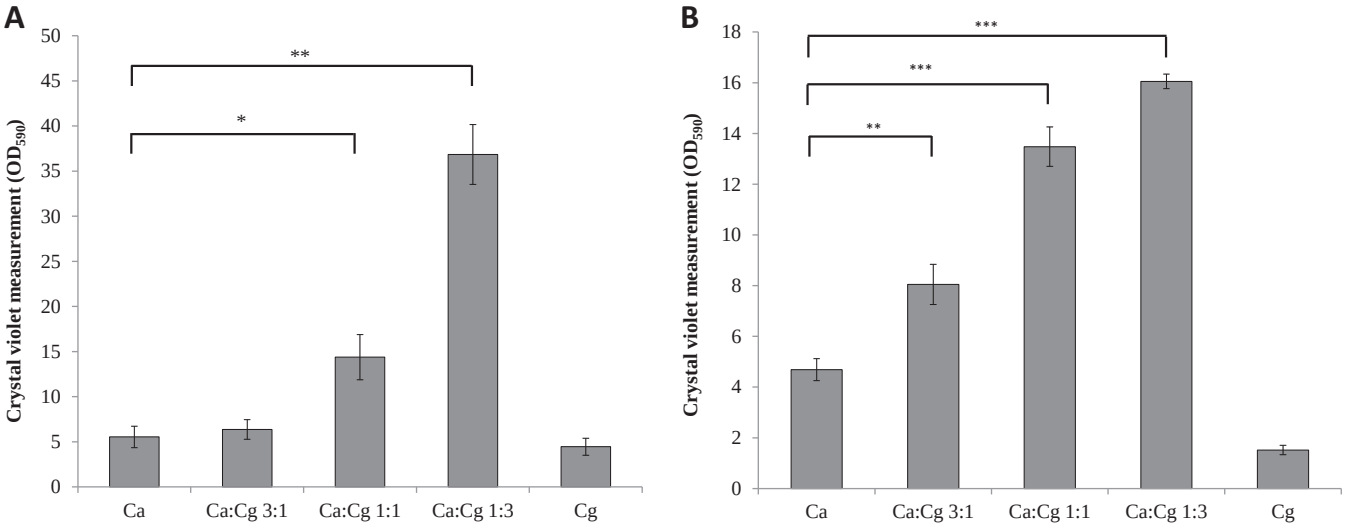

FIG 1 Effect of starting culture composition on *Candida* coculture biofilm formation. Biofilms formed on glass coverslips (A) or polystyrene microtiter plates (B) for 48 h. Four biological replicates. Ca, *C. albicans*; Cg, *C. glabrata*; *, $P < 0.05$; **, $P < 0.01$; ***, $P < 0.001$ compared with *C. albicans* monoculture by Student's *t* tests. Error bars are standard errors of samples.

to biofilm formation and pathogenesis. In this work, we investigated the effect of how changing the initial *C. albicans* and *C. glabrata* ratio impacts biofilm formation and structure and antifungal drug susceptibility.

RESULTS

Increasing *C. glabrata* in a *Candida* coculture increases biofilm formation. We investigated the effect of changing the initial ratio of *C. albicans* to *C. glabrata* on biofilm formation on glass surfaces. Figure 1 shows that the extent of biofilm formation after 48 h of culture was significantly impacted by the starting ratio of *C. albicans* to *C. glabrata* at the three ratios tested (3:1, 1:1, and 1:3). *C. albicans* and *C. glabrata* monocultures demonstrated comparable biofilm biomass formations on glass surfaces, as determined by crystal violet staining (Fig. 1A). However, on polystyrene and acrylic surfaces, biofilm formation by *C. glabrata* monocultures was lower than that of *C. albicans* monocultures (Fig. 1B; see also Fig. S1 in the supplemental material). Interestingly, while *C. glabrata* monocultures showed lower biofilm formation than *C. albicans* on a polystyrene surface, increasing the initial cell density of *C. glabrata* in the mixed-species biofilm led to an increase in total biofilm formation (see Fig. 1B). A ratio of 1:3 (*C. albicans* to *C. glabrata*) yielded the maximum biofilm growth, which was significantly higher than those observed with both *C. albicans* monocultures and 3:1 and 1:1 initial ratios of *C. albicans*/*C. glabrata* cocultures. No additional increase in biofilm formation was observed when the ratios of *C. albicans* to *C. glabrata* were increased to 1:5 and 1:10 (see Fig. S2).

We quantified the numbers of *C. albicans* and *C. glabrata* cells in the coculture biofilms to determine whether one species was more abundant in the biofilm. Our results showed that the ratio of *C. albicans* to *C. glabrata* in mature biofilms after 48 h remained approximately similar to the initial inoculum ratio (see Fig. S3), suggesting that one species does not have a significant fitness advantage over the other under the culture conditions that were used.

Since hyphae and biofilm formations in *C. albicans* increase under nutrient-limited conditions (33, 34), it may be possible that the increase in biofilm biomass observed in cocultures is the result of nutrient competition in *C. albicans*/*C. glabrata* cocultures. As a control experiment, cocultures of *C. albicans* and *Saccharomyces cerevisiae* were used to mimic the nutrient competition environment of cocultures to ensure that the enhanced biofilm formation observed in *C. albicans*/*C. glabrata* cocultures is the result of potential interactions between *C. albicans* and *C. glabrata* and not due to nutrient-

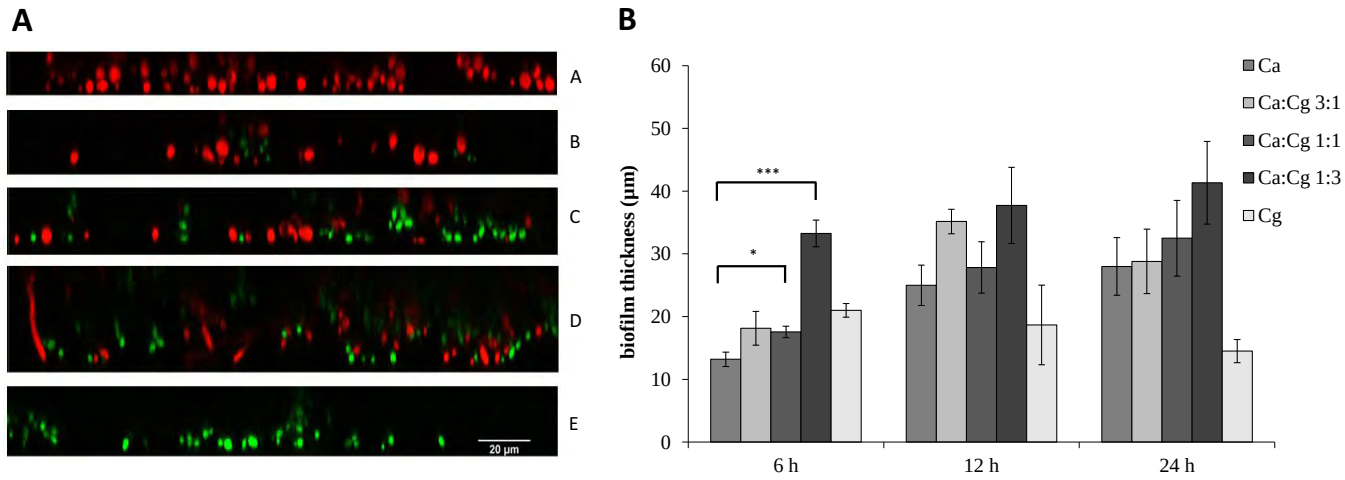

FIG 2 Confocal microscopy analysis of *Candida* coculture biofilm thickness. (A) Representative 6-h 3D *Candida* biofilm cross-sectional views. Red, *C. albicans*; green, *C. glabrata*; A, *C. albicans*; B, *C. albicans*/*C. glabrata* 3:1; C, *C. albicans*/*C. glabrata* 1:1; D, *C. albicans*/*C. glabrata* 1:3; E, *C. glabrata*. (B) Biofilm thickness at 6, 12, and 24 h. Student's *t* test, *, $P < 0.05$; ***, $P < 0.001$ compared with *C. albicans* monoculture. Error bars are standard errors from 3 biological replicates.

limited conditions experienced by *C. albicans* in cocultures. The data show that unlike the *C. albicans*/*C. glabrata* cocultures, the biofilm formation with *C. albicans*/*S. cerevisiae* 1:3 cocultures was not greater than monocultures of *C. albicans* or *S. cerevisiae* (see Fig. S4), suggesting that the enhanced biofilm formation observed in *C. albicans*/*C. glabrata* cocultures was not due to nutrient competition.

Increased *C. albicans* hyphae and biofilm structural heterogeneity in *Candida* coculture biofilms. The composition and structure of *Candida* coculture biofilms were characterized using confocal laser scanning microscopy (CLSM). Biofilms were imaged 6, 12, and 24 h after the initiation of cocultures to assess the differences in biofilm compositions and structures between various initial *C. albicans*/*C. glabrata* ratios. The biofilm images were used to reconstruct the three-dimensional (3D) structures of mono- and coculture biofilms. An image analysis revealed long *C. albicans* hyphae throughout the *C. albicans*/*C. glabrata* 1:3 coculture biofilms and an increased biofilm thickness compared to those under the other culture conditions during the early biofilm maturation phase after just 6 h of growth (Fig. 2A and B). Moreover, the thicknesses of coculture biofilms at *C. albicans*/*C. glabrata* ratios of 1:1 and 1:3 were significantly higher than those of *C. albicans* monoculture biofilms at 6 h (*P* values of 0.05 and 0.001, respectively) (Fig. 2B). After 12 h, the coculture biofilm thicknesses were comparable in all three *C. albicans*/*C. glabrata* ratios but still greater than those of *C. albicans* monoculture biofilms (Fig. 2B). The reconstructed 3D biofilms also revealed extensive heterogeneity in the *C. albicans*/*C. glabrata* 1:3 cocultures, which differed from the other two ratios tested. In the *C. albicans*/*C. glabrata* 1:3 biofilm, there was increased clustering of *C. albicans* hyphae and *C. glabrata* yeast cells as well as variations in biofilm structure and thickness over the entire surface of the biofilm. Interestingly, the thicknesses of *C. albicans*/*C. glabrata* 1:3 biofilms varied across the entire surface of the biofilms, revealing a more heterogeneous biofilm topology; whereas the thicknesses of *C. albicans*/*C. glabrata* 3:1 and 1:1 biofilms were more uniform across the entire biofilms (Fig. 3A; see also Fig. S5 and S6). The lengths of *C. albicans* hyphae were estimated from the reconstructed 3D biofilms. At each time point, hypha lengths increased significantly with increasing *C. glabrata* concentrations in the coculture biofilms, with the *C. albicans*/*C. glabrata* 1:3 biofilm exhibiting the longest hyphae at all three time points (Fig. 3B).

C. albicans monoculture biofilms were thinner than coculture biofilms and were composed of both yeast and hyphal cells in dense mats that were tightly interwoven as evident by the close clustering of red in the representative images (Fig. 3A; see also Fig. S5 to S7). *C. glabrata* monoculture biofilms were composed of yeast cells, but the

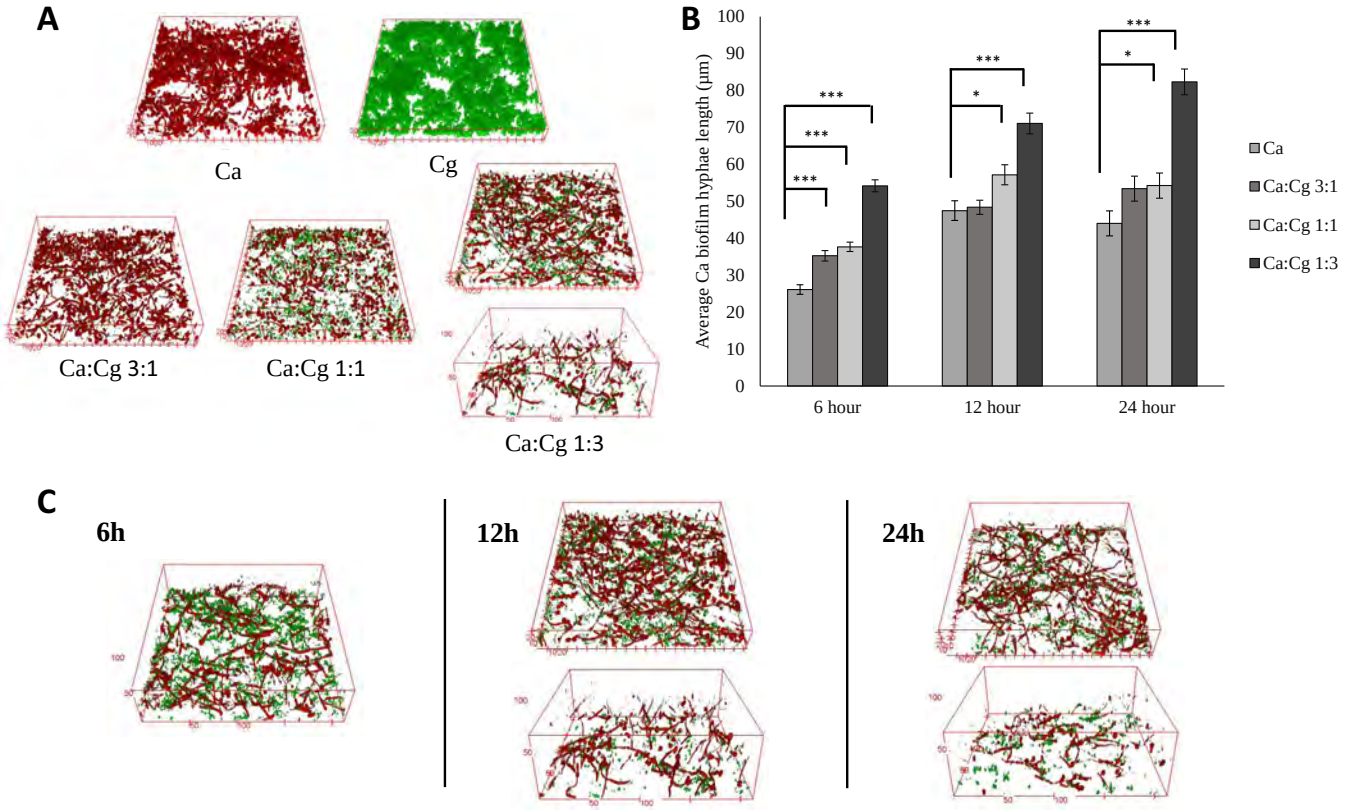

FIG 3 Effect of culture composition on biofilm structure. (A) Representative 12-h 3D biofilm. Scale bars in microns. (B) Average *C. albicans* hyphal length in biofilms. (C) Representative 3D biofilm images of *C. albicans*/*C. glabrata* 1:3 at 6, 12, and 24 h. Scale bar in microns. Student's *t* test, *, $P < 0.05$; ***, $P < 0.001$ compared with *C. albicans* monoculture. Error bars are standard errors from 3 biological replicates.

yeast cells formed small clusters that contributed to a thin biofilm layer (Fig. 2A; Fig. S5 to S7). However, coculture biofilms with an initial *C. albicans*/*C. glabrata* ratio of 1:3 demonstrated different characteristics. Two distinct features were observed: a dense, but not thick, region that comprised a mat of *C. albicans* hyphae and *C. glabrata* cells and a less dense, but thicker, region with long and elongated *C. albicans* hyphae that contributed to the increased thickness and volume, with few *C. glabrata* cells (Fig. 3A and C). The denser regions of the *C. albicans*/*C. glabrata* 1:3 biofilm were similar to those observed with *C. albicans* monoculture biofilms or coculture biofilms started with *C. albicans*/*C. glabrata* at 1:1 and 3:1 ratios (Fig. 3A; Fig. S5 and S6).

In addition to increased thicknesses and *C. albicans* hypha lengths in the *Candida* coculture biofilms, the observed physical associations between *C. albicans* and *C. glabrata* in the mixed-species biofilm were quantified. *C. glabrata* appears to preferentially attach to a hypha of *C. albicans* (Fig. 4A to C), which was previously observed (29). The clustering between the two *Candida* species was most abundant in the *C. albicans*/*C. glabrata* 1:3 biofilm, where the percentage of *C. glabrata* cells attached to *C. albicans* hyphae was significantly higher than those from the *C. albicans*/*C. glabrata* 3:1 coculture at 12 and 24 h and the *C. albicans*/*C. glabrata* 1:1 ratio at 6 and 12 h (Fig. 4D).

Gene expression analysis of adhesion genes in *C. albicans* biofilms. Reverse transcription-quantitative PCR (qRT-PCR) was utilized to analyze gene expression at 6, 12, and 24 h in all *C. albicans*/*C. glabrata* coculture biofilms. For *C. albicans*, four adhesion and invasion associated genes (*HWP1*, *ALS3*, *PLB5*, and *SAP9*) were chosen, whereas two *C. glabrata* adhesion genes (*EPA1* and *EPA6*) were chosen as representative *C. glabrata* genes (Table 1). *HWP1*, *ALS3*, *PLB5*, and *SAP9* are all genes that contribute to *C. albicans* cell wall integrity and adhesion during biofilm formation. In *C. glabrata*, *EPA1* and *EPA6* are known

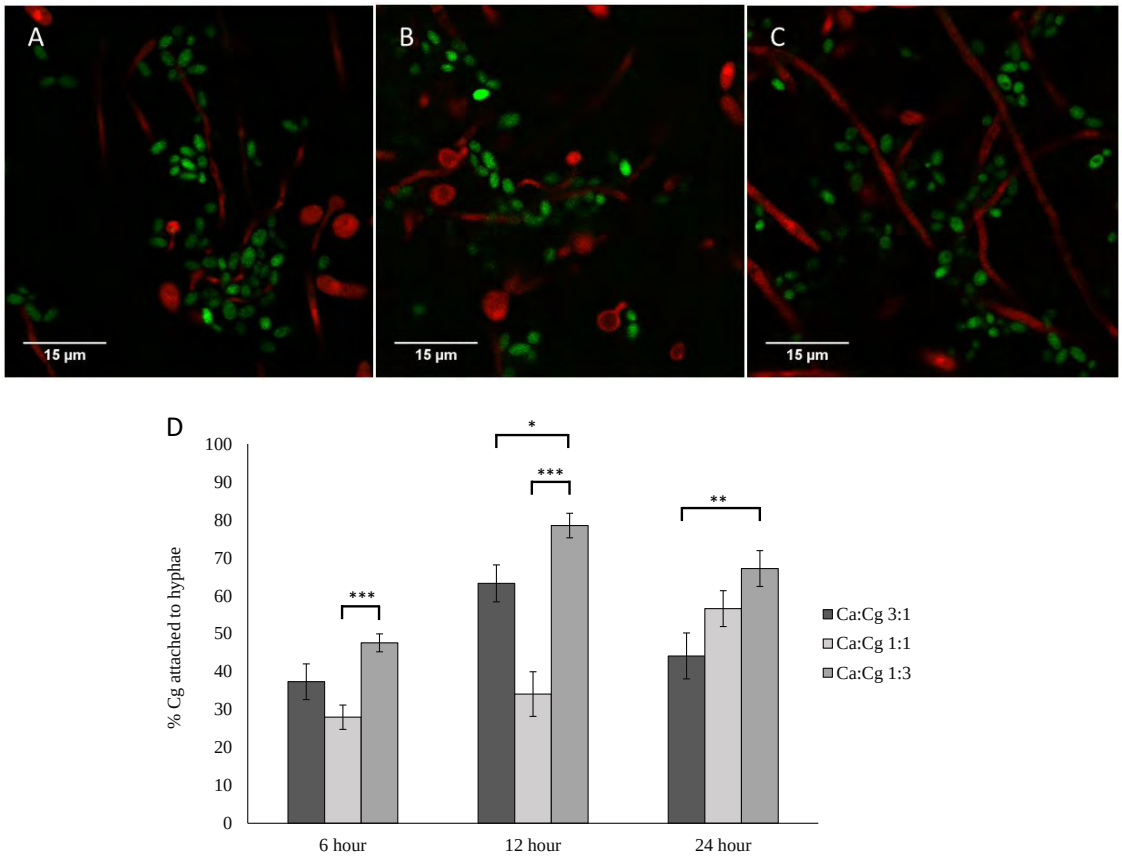

FIG 4 Physical association of *C. glabrata* with *C. albicans* hyphae in biofilms. (A) *C. albicans*/*C. glabrata* 3:1. (B) *C. albicans*/*C. glabrata* 1:1. (C) *C. albicans*/*C. glabrata* 1:3. (D) Percent *C. glabrata* attached to *C. albicans* hyphae in *Candida* coculture biofilms. Student's *t* test, *, $P < 0.05$; **, $P < 0.01$; ***, $P < 0.001$ compared with *C. albicans* monoculture. Error bars are standard errors from 3 biological replicates.

adhesion genes that have been demonstrated to be upregulated in biofilms (35). All of these genes were previously reported to be involved in biofilm formation and *Candida* virulence (36–40). The expression of *HWP1* increased with increasing *C. glabrata* in the coculture biofilm. The maximum increase in *HWP1* expression was observed at 12 h and

TABLE 1 qRT-PCR primer list

Gene	Primer sequence (5′→3′)[a]
C. albicans	
HWP1	F, TTGGCTAGTGAAACCTCACCAA
	R, GGCAGATGGTTGCATGAGTG
ALS3	F, ACTTTGTGGTCTACAACTTGGG
	R, CCAGATGGGGATTGTAAAGTGG
PLB5	F, CATTTGACTCGTCCGGCTCT
	R, ATGATGCCTGGGCAGAGGA
SAP9	F, TGTAACTTGGCCGACTCCAG
	R, ACGAGCTTGACGATTGTTGCAT
ADH1	F, TGGGTGCTGAAGCTTACGTT
	R, TGACTTTAGCGTGAGCTGGT
C. glabrata	
EPA1	F, ACCTAGCCCATACGGACCAA
	R, TCTGAGAAAGCATACTCGCTTGA
EPA6	F, TCCGAATTATCCTCGAACAGGC
	R, ATCAAACAGCGAAGTACACCC
ADH1	F, GAGCCGTCTTCCCTTCCA
	R, CGTGTTCGATTCGGTAACGC

[a]F, forward; R, reverse.

TABLE 2 Relative *C. albicans* biofilm gene expression

Gene	*C. albicans*/*C. glabrata* ratio biofilm	Gene expression level (relative to *ADH1*)[a] after:		
		6 h	12 h	24 h
HWP1	*C. albicans* monoculture	0.352 ± 0.262	1.274 ± 0.280	0.151 ± 0.102
	3:1	0.357 ± 0.148	1.070 ± 0.330	0.465 ± 0.098
	1:1	0.680 ± 0.237	2.141 ± 0.822	0.621 ± 0.114*
	1:3	0.774 ± 0.157	3.827 ± 0.369**	0.829 ± 0.095**
ALS3	*C. albicans* monoculture	0.095 ± 0.053	0.359 ± 0.103	0.052 ± 0.021
	3:1	0.146 ± 0.075	0.238 ± 0.065	0.157 ± 0.019*
	1:1	0.257 ± 0.089	0.345 ± 0.088	0.177 ± 0.055
	1:3	0.337 ± 0.052*	0.714 ± 0.084	0.163 ± 0.007*

[a]Values are averages ± standard errors from 3 biological replicates with 3 technical replicates each. Statistical significance determined by Student's *t* tests with respect to *C. albicans* monoculture biofilm: *, $P < 0.05$; **, $P < 0.01$.

was significantly different between *C. albicans* monoculture biofilms and coculture biofilms at 3:1 and 1:3 ratios (*t* test, $P < 0.01$). At 24 h, *HWP1* gene expression in *C. albicans*/*C. glabrata* 1:1 and *C. albicans*/*C. glabrata* 1:3 was significantly higher than in the *C. albicans* monoculture biofilm (Table 2).

ALS3 gene expression increased as the ratio of *C. albicans* to *C. glabrata* decreased, and the maximum increase was again observed at 12 h. *ALS3* gene expression was significantly higher in the *C. albicans*/*C. glabrata* 3:1 biofilm at 24 h and in the *C. albicans*/*C. glabrata* 1:3 biofilm at 6 and 24 h than in the *C. albicans* monoculture biofilm (*t* test, $P < 0.05$) (Table 2). The expression of *PLB5* did not change significantly between *C. albicans* and the coculture biofilms at all ratios at the three time points, whereas *SAP9* gene expression decreased at all time points in the coculture biofilms compared to that in the *C. albicans* monoculture (see Table S1). The expression of *C. glabrata* adhesion genes *EPA1* and *EPA6* was unchanged at all ratios and time points compared to that in the *C. glabrata* monoculture (Table 3).

***Candida* coculture biofilms demonstrate increased antifungal resistance.** As biofilm formation is known to increase antimicrobial drug resistance (24, 28, 41), the increased biofilm thickness and structural complexity of *C. albicans*/*C. glabrata* cocultures can potentially result in enhanced antifungal drug resistance. Therefore, the impact of the *C. albicans*/*C. glabrata* ratio on the susceptibility of *C. albicans* and *C. glabrata* biofilm cultures to caspofungin was tested. The MIC_{50}s for the planktonic culture of *C. glabrata* and the mixed *C. albicans*/*C. glabrata* 1:1 coculture were each measured to be 0.0156 μg/ml, which was double that of the *C. albicans* monoculture (0.0078 μg/ml), and the MIC_{90}s were 0.0312 μg/ml for all conditions. The MIC_{50} and MIC_{90} of planktonic *Candida* cultures were lower than those observed in biofilms (see Table S2).

Due to differences in the metabolism of 2,3-bis-(2-methoxy-4-nitro-5-sulfophenyl)-2H-tetrazolium-5-carboxanilide salt (XTT) between *Candida* species, CLSM was utilized for cell enumeration and to quantify cell viability of caspofungin-treated biofilms. A caspofungin concentration of 0.03 μg/ml was chosen to analyze cell viability on the basis of unpublished data from our laboratory showing that the MIC_{50} using the XTT assay was 0.03 μg/ml for *C. albicans*, *C. glabrata*, and coculture biofilms (Table S2). After caspofungin treatment, the *C. glabrata* monoculture biofilm had a viability of 14% ± 2.5% and the *C. albicans* monoculture biofilm was 43% ± 4.4% viable compared to untreated control biofilms (Fig. 5). In coculture biofilms, the total cell viability increased with increasing *C. glabrata* in the biofilm. The *C. albicans*/*C. glabrata* 1:3 biofilm had a cell viability of 75% ± 8.4%, which was significantly higher than those of the *C. albicans*/*C. glabrata* 3:1 and *C. albicans*/*C. glabrata* 1:1 biofilms, which exhibited viabilities of 37% ± 8.2% and 62% ± 5.7%, respectively (Fig. 5). When considering the individual species viability in coculture biofilms, *C. albicans* was more susceptible to caspofungin than *C. glabrata*. In the mixed-species biofilm, *C. glabrata* continued to grow even after the addition of caspofungin.

TABLE 3 Relative *C. glabrata* biofilm gene expression

Gene	*C. albicans*/*C. glabrata* ratio biofilm	Gene expression level (relative to *ADH1*)[a] after:		
		6 h	12 h	24 h
EPA1	*C. glabrata* monoculture	0.026 ± 0.005	0.032 ± 0.011	0.078 ± 0.023
	3:1	0.014 ± 0.004	0.040 ± 0.014	0.197 ± 0.063
	1:1	0.013 ± 0.003	0.049 ± 0.008	0.256 ± 0.098
	1:3	0.011 ± 0.002	0.048 ± 0.015	0.192 ± 0.074
EPA6	*C. glabrata* monoculture	0.442 ± 0.201	0.407 ± 0.211	0.256 ± 0.149
	3:1	0.635 ± 0.268	0.676 ± 0.447	0.380 ± 0.234
	1:1	0.510 ± 0.175	0.980 ± 0.656	0.402 ± 0.266
	1:3	0.430 ± 0.243	0.360 ± 0.193	0.346 ± 0.162

[a]Values are averages ± standard errors from 3 biological replicates with 3 technical replicates each.

DISCUSSION

Recent microbiome studies have started to shed light on how the composition of bacterial and fungal species can potentially correlate with health and disease (32, 42–44). *Candida*, being a commensal fungal microorganism and opportunistic pathogen (10), is involved in this paradigm of health and disease. As *Candida* species exhibit variable susceptibility to antifungal treatments, a changing prevalence of *Candida* spp. in candidiasis and candidemia on an epidemiological level (45–47) and changing colonization of fungal species over time at the single patient level have been observed (45, 48, 49), suggesting there are changes in the mycobiome during the course of disease and treatment. *Candida* biofilms pose a high risk to human health, as high rates of infection and mortality are correlated with biofilm formation due to the enhanced resistance to antimicrobials (50). Clinical studies show that *C. albicans* and *C. glabrata* are often coisolated in infections (45, 51, 52), and the degree of infection is worsened by the presence of both species (20, 53). While the clinical importance of *Candida* spp. in biofilms is evident, the interactions between *C. albicans* and *C. glabrata*, in terms of their relative abundances and their effects on the development of *Candida* biofilms, are poorly understood. In this work, we investigated the impacts of changing the relative starting ratios of *C. albicans* and *C. glabrata* in coculture biofilms on biofilm formation and the resistance to antifungal treatment. Our results clearly demonstrate that the relative abundance of each species has a significant impact on biofilm formation, as biofilms increased with increased levels of *C. glabrata*. This observation is especially interesting as we and others (54–57) have shown that *C. glabrata* in monocultures forms a weaker biofilm than *C. albicans*. The fact that this density-dependent effect was

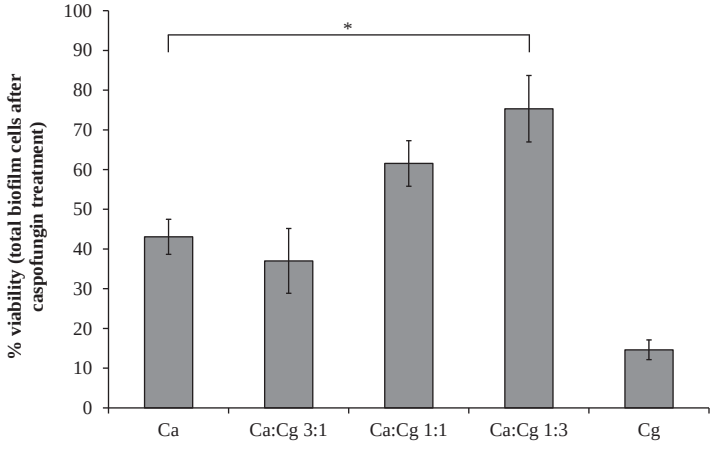

FIG 5 *Candida* biofilm viability after caspofungin treatment. Student's *t* test, *, $P \leq 0.05$ compared to *C. albicans* monoculture. Error bars are standard errors from 3 biological replicates.

observed with biofilms grown on different surfaces (glass, polystyrene, and acrylic) suggests that this behavior is independent of the surface characteristics.

An analysis of biofilms using CLSM revealed that the ratios of *C. albicans* to *C. glabrata* remained relatively constant at the levels in which they were seeded over the duration of the experiment. This suggests that one species did not have a nutritional or metabolic advantage to outgrow the other in the biofilm (see Fig. S3 in the supplemental material). Cataldi et al. (58) demonstrated that a complex biofilm structure (biofilm composed of blastospores and pseudohyphal and hyphal cells) increased the biofilm cell surface area, which can increase adhesion to host cell surfaces and pathogenesis. Recently, Alonso et al. demonstrated that macrophage migration toward *C. albicans*, a mechanism for clearing infection and pathogens in the human body, is reduced 2-fold when cells are in a biofilm, which was attributed to increased biofilm thickness and structure (extracellular matrix encasement of yeast and hyphal cells [59]), rather than the composition of the biofilm matrix (60). In this work, we also observed increased structural complexity and heterogeneity in coculture *Candida* biofilms compared to those of monoculture biofilms, where the highest biofilm heterogeneity was seen in the *C. albicans*/*C. glabrata* 1:3 biofilm. The increase in structural complexity was evident from the increase in *C. albicans* hypha formation and uneven thickness across the biofilm, which resulted in a larger network of cells and more complex 3D structure (Fig. 2 and 3; Fig. S5 to S7).

Because of the increase in hyphae and uneven topology, the overall biofilm thickness was not an appropriate metric for quantifying coculture *Candida* biofilms. Instead, 3D biofilm reconstructed images were used for biofilm data interpretation. For example, the increase in hypha length observed with the 1:3 *C. albicans*/*C. glabrata* biofilms suggests that the *C. albicans*/*C. glabrata* 1:3 biofilm is potentially more virulent than 1:1 or 3:1 ratio biofilms, as an increase in hypha length is often associated with increased *C. albicans* virulence (34). We observed that a majority of *C. albicans* yeast cells were on the bottom of the biofilm with hyphal cells growing upward (Fig. 2; Fig. S7), which is similar to the observations reported by Kuhn et al. with monoculture *C. albicans* biofilms (61). In our observations of *C. albicans*/*C. glabrata* coculture biofilms, *C. glabrata* was evenly dispersed throughout the biofilm, and aggregates formed around *C. albicans* hyphae (Fig. 3C and 4). While clustering of *C. glabrata* around *C. albicans* hyphae was seen in all three *C. albicans*/*C. glabrata* ratios (Fig. 4A to C), maximal clustering was observed in the *C. albicans*/*C. glabrata* 1:3 biofilm. This observation is consistent with the longer hyphae that were observed in this coculture condition (Fig. 3B).

Previous studies have shown that several *C. albicans* genes (e.g., *HWP1* and *ALS3*) and *C. glabrata* genes (e.g., *EPA1* and *EPA6*) are involved in increased adhesion and biofilm formation *in vitro* and *in vivo* (37, 39, 40). In this study, the expression of both *HWP1* and *ALS3* increased in the coculture biofilms compared to that in a *C. albicans* monoculture biofilm, and the highest fold induction was observed with the starting ratio of *C. albicans* to *C. glabrata* of 1:3 (Table 2). The increase in *HWP1* gene expression for the *C. albicans*/*C. glabrata* 1:3 biofilm is consistent with the increased hypha length seen in the biofilms (Fig. 3B), as *HWP1* (hyphal wall protein 1) is a *C. albicans* hypha-associated gene involved in adhesion and invasion (62, 63). *ALS3* gene expression was highest in *C. albicans*/*C. glabrata* 1:3 coculture biofilms compared to that in *C. albicans* monoculture biofilms at 6 and 24 h, indicating that Als3 may be needed for the initial formation of *Candida* coculture biofilms (at 6 h) and also for the maintenance of a mature biofilm structure (at 24 h). Early activation of *ALS3* gene expression in *C. albicans* biofilms was previously demonstrated by Nailis et al., where *ALS3* gene expression increases within 6 h compared to that in planktonic cells and then is downregulated after 48 h (64). The increased expression of *C. albicans* cell wall adhesins *HWP1* and *ALS3* also suggests an increase in the attachment of cells within the biofilm, which enables more robust biofilm formation than in biofilms with lower adhesin expression. Moreover, increased hyphae in *C. albicans* and increased *HWP1* expression are associated with increased yeast-hypha cell interactions in the biofilm, which contributes to the

increased structural complexity of cells within the biofilm matrix (Fig. 4D), and *ALS3* has been demonstrated to facilitate the binding of *C. glabrata* to *C. albicans* in a biofilm, further leading to biofilm robustness and thickness in coculture (29). The expression of *HWP1* and *ALS3* is also activated earlier on in the *C. albicans*/*C. glabrata* 1:3 biofilm than in the *C. albicans* monoculture, indicating an earlier initiation of biofilm formation, which possibly contributes to the higher biomass seen over time with the 1:3 ratio.

We observed an increase in the expression of the *C. glabrata* adhesion gene *EPA1* at 24 h in coculture biofilms. Recently, Tati et al. demonstrated that several *EPA* adhesions genes (*EPA8* and *EPA19*) are upregulated in mixed-species cultures of *C. albicans* and *C. glabrata* (29). While no significant change in the expression of *EPA1* or *EPA6* was observed between coculture and monoculture biofilms (Table 3), it should be noted that *EPA1* has been primarily reported to be involved in adhesion to host tissue (40), and the lack of an observed gene expression change in *EPA1* and *EPA6* could also be the result of subtelomeric silencing (65–67).

In concordance with the biofilm data, *C. albicans*/*C. glabrata* 1:3 coculture biofilms exhibited the highest resistance to caspofungin treatment (Fig. 5). Cataldi et al. (58) reported that a nonuniform biofilm has an increased susceptibility to antifungal drugs due to a lower biofilm cell-matrix density and discontinuous cell embedding in the extracellular matrix, which could explain the increased resistance to caspofungin with the *C. albicans*/*C. glabrata* 1:3 biofilm. Interestingly, while *C. albicans* monoculture biofilms were more susceptible to caspofungin, *C. glabrata* biofilm cells in coculture grew in the presence of 0.03 μg/ml caspofungin (Fig. S3). It is unclear why *C. glabrata* cell viability increases in coculture biofilms in the presence of caspofungin and whether this phenomenon is observed for other antifungal drugs as well.

Our study presents multiple lines of evidence to demonstrate that the initial relative cell densities of *C. albicans* and *C. glabrata* in a coculture biofilm strongly influence the extent of biofilm formation as well as its structural complexity. The increased hypha length in the *C. albicans*/*C. glabrata* 1:3 biofilm contributes to a more complex biofilm structure, which increases the thickness and antifungal resistance of the biofilm. Additionally, increased hyphae also provide more hyphal surface area for *C. glabrata* yeast cells to attach and cluster in the biofilm. These observations suggest that the changing *Candida* polymicrobial culture dynamics during biofilm formation may alter the course of the infection. Ongoing work in our laboratory is focused on investigating the transcriptomic changes in coculture biofilms and identifying the molecular basis underlying *Candida* interspecies interactions.

MATERIALS AND METHODS

Microorganisms and growth conditions. *C. albicans* (SC5314, J. Berman, ENO1-RFP::Nat1) (68) and *C. glabrata* (ATCC 2001, green fluorescent protein [GFP] labeled) were used in this study. Prior to the experiments, the strains were cultured on yeast extract-peptone-dextrose (YPD) agar plates for 48 h at 30°C. For all experiments, single colonies were isolated from YPD agar plates and inoculated in 25 ml yeast nitrogen base (YNB) medium (50 mM glucose, pH 7; Amresco). Cultures were grown for 12 h at 30°C and 170 rpm prior to experiments.

Biofilm quantification assay. Biofilms were grown in either 96-well polystyrene plates (Corning) or on glass or acrylic coverslips (VWR) in 6-well tissue cultures plates. The 96-well plates or coverslips were incubated in heat-inactivated fetal bovine serum (HI FBS) overnight at 37°C. Prior to the experiment, coverslips or wells were washed once in 1× phosphate-buffered saline (PBS; pH 7.4), and the coverslips were placed into 6-well tissue culture plates. Overnight cultures were washed twice with PBS and resuspended in fresh YNB medium. A hemocytometer was used for the calculation of cell density, and cell cultures were diluted to a final concentration of 10^7 cells/ml. A final volume of 4 ml cell culture was added to each well with a coverslip, and 100 μl was added to the 96-well plates. Wells with medium only were used as the controls. Biofilms were allowed to grow at 37°C for 48 h without agitation. After 48 h, the coverslips were removed from the 6-well plates using tweezers and washed twice with PBS. For the 96-well plates, wells were washed twice with 200 μl PBS. Coverslips were placed in a new 6-well plate, where 2 ml (200 μl for microtiter plates) of 99% methanol was added to each biofilm. After 15 min, excess methanol was removed from the wells and biofilms were allowed to dry completely. Once dry, 2 ml (200 μl for microtiter plates) of 0.1% crystal violet was added to each biofilm and incubated at room temperature for 20 min (69). Plates were rinsed gently with deionized water to remove excess crystal violet stain from the wells and biofilms. Excess water was removed from the wells, and 1 ml (150 μl for microtiter plates) of 33% acetic acid was added to each biofilm. Acetic acid samples were diluted 50-fold

in a black-walled clear-bottom 96-well Corning plate, and the absorbance was measured at 590 nm in a plate reader (Molecular Devices SpectraMax 340PC).

Confocal laser scanning microscopy. For CLSM biofilm analysis, biofilms were grown in 2-well chambered cover glass slides (Nunc Lab-Tek) that were preincubated overnight with HI FBS at 37°C. Cultures of *C. albicans* and *C. glabrata* were grown overnight in YNB medium. Cultures were washed twice in PBS and adjusted to a cell density of 10^7 cells/ml. A final volume of 2 ml per well was used. Biofilms were allowed to grow for 48 h at 37°C without agitation. After 48 h of growth, biofilms were washed gently with PBS and fixed with 4% paraformaldehyde (at room temperature in the dark for 30 min). Images were acquired on a Zeiss LSM 780 NLO multiphoton microscope (Zeiss, USA) using the Plan-Apo 40×/1.4 oil differential interference contrast (DIC) M27 objective with 488 nm and 543 nm laser lines to image GFP and red fluorescent protein (RFP) simultaneously. To analyze the structures of the biofilms, a series of optical sections were taken at 1-μm intervals throughout the depths of the biofilms. Three biological replicates were imaged and up to 3 images were taken per biofilm sample and used in both Comstat2 and ImageJ analyses. Image J (70) was used to adjust the brightness of images, render 3D image stacks, and quantify hypha length and cell clustering. Comstat2 (71, 72) was used for calculating biofilm thickness.

RNA extraction and qRT-PCR analysis. As described above, biofilms were grown for 6, 12, and 24 h on glass coverslips in 6-well tissue culture plates. Biofilms were washed off the coverslips with prechilled sterile Millipore water, and the cells were collected by centrifugation (2,000 × *g* for 5 min at 4°C). The supernatants were removed and cell pellets were flash-frozen in liquid nitrogen prior to placing in a lyophilizer for drying. The cell pellets were allowed to dry for 24 h. Acid-washed glass beads (Sigma-Aldrich) were added to the dried cell pellets, which were disrupted in a Disruptor Genie by using 2-min cycles for up to 10 min. Lysis buffer from the GE Illustra RNAspin minikit was added to the disrupted cell powder, and RNA was extracted using the kit protocol with on-column DNase I treatment. RNA quality and concentration were determined using a Nanodrop and Qubit, respectively.

For qRT-PCR, a qScript one-step SYBR green qRT-PCR kit (Quanta Biosciences) was used in a Roche LightCycler 96 system. Fifty nanograms of RNA was used in each reaction mixture. *ADH1* was the reference gene used for ΔC_T analysis. For $\Delta\Delta C_T$ analysis, the monoculture biofilm ΔC_T was subtracted from the coculture biofilm ratios. A $2^{-\Delta\Delta CT}$ analysis was used to determine the fold change in gene expression. Standard deviations were taken from $2^{-\Delta\Delta CT}$ values of three biological replicates. The primers used are listed in Table 1.

Antifungal susceptibility test. Caspofungin (GoldBio, St. Louis, MO) was dissolved in sterile Milli-Q water to a concentration of 1 mg/ml. The caspofungin stock solution was stored at −80°C in individual aliquots for one-time use. The CLSI M27-A2 (73) testing standard was slightly modified and used to test *Candida* planktonic caspofungin susceptibility. The cells were diluted to a concentration of 5.0×10^2 to 2.5×10^3 cells/ml in YNB medium (50 mM glucose, pH 7). The cultures were allowed to grow for 48 h in test tubes at 37°C without agitation. The optical density at 600 nm (OD_{600}) of planktonic cultures was measured after 48 h. To test biofilm susceptibility, 96-well microtiter plates were coated with HI FBS and placed at 37°C overnight. The wells were washed once with PBS before inoculating with prepared cell cultures as mentioned above. The final volume in the wells was 100 μl. Biofilms were allowed to grow for 24 h at 37°C. After 24 h, the biofilms were washed twice with 200 μl PBS, and fresh YNB medium or YNB medium with caspofungin was added to the wells. The plates were placed back at 37°C for 24 h. After 48 h of total growth, the biofilms were washed twice with 200 μl PBS and processed with either the XTT assay or CLSM for biofilm cell counts.

The quantitation of *Candida* biofilms was performed as described previously (74, 75) using both a biochemical assay, the XTT reduction assay, and CFU measurements via confocal microscopy. XTT is reduced by mitochondrial dehydrogenase into a water-soluble formazan product that is measured spectrophotometrically. Briefly, XTT (Sigma Chemical Co. [St. Louis, MO] or Amresco) was dissolved in PBS to a final concentration of 0.5 mg/ml and filter sterilized. Menadione (Spectrum, NJ) was dissolved in acetone to a final concentration of 10 mM. XTT and menadione aliquots were stored at −80°C for future use. The menadione solution was added to the XTT solution for a final concentration of 1 μM. One hundred microliters of the XTT-menadione solution was added to the wells, and the plates were wrapped in foil and incubated at 37°C for 3 h. Eighty microliters of the supernatant was added to a new 96-well plate and measured at 490 nm (Tecan Infinite M200). The percent viability was calculated using the following equation: percent viability = $100 \times (A_{490}$ treated $- A_{490}$ background$)/(A_{490}$ untreated $- A_{490}$ background).

To count biofilm cells from the antifungal susceptibility test, cells were removed from the 96-well plates by the addition of 100 μl PBS and scraped with a pipette tip. A total of 3 technical replicates were collected and combined for one sample in a microcentrifuge tube. The samples were vortexed vigorously and 10 μl of cell suspension was added to a coverslip and imaged. Images were taken using a Leica TCS SP5 (Leica, Germany) using an HCX Plan-Apo 40×/0.85 dry objective with 488 nm and 543 nm laser lines with a 1.7× zoom. Ten images were taken per sample, and cell counts from a total of 3 biological replicates were counted using Image J software (70).

SUPPLEMENTAL MATERIAL

Supplemental material for this article may be found at https://doi.org/10.1128/AEM.02769-17.

SUPPLEMENTAL FILE 1, PDF file, 0.9 MB.

ACKNOWLEDGMENT

This work was supported in part by the Nesbitt Chair Endowment to A.J. and NSF MCB-1054276 to K.C.K.

REFERENCES

1. Underhill DM, Iliev ID. 2014. The mycobiota: interactions between commensal fungi and the host immune system. Nat Rev Immunol 14:405–416. https://doi.org/10.1038/nri3684.
2. Cho I, Blaser MJ. 2012. The human microbiome: at the interface of health and disease. Nat Rev Genet 13:260–270. https://doi.org/10.1038/nrg3182.
3. Bansal T, Alaniz RC, Wood TK, Jayaraman A. 2010. The bacterial signal indole increases epithelial-cell tight-junction resistance and attenuates indicators of inflammation. Proc Natl Acad Sci U S A 107:228–233. https://doi.org/10.1073/pnas.0906112107.
4. Berg RD. 1996. The indigenous gastrointestinal microflora. Trends Microbiol 4:430–435. https://doi.org/10.1016/0966-842X(96)10057-3.
5. Claesson MJ, Jeffery IB, Conde S, Power SE, O'Connor EM, Cusack S, Harris HM, Coakley M, Lakshminarayanan B, O'Sullivan O, Fitzgerald GF, Deane J, O'Connor M, Harnedy N, O'Connor K, O'Mahony D, van Sinderen D, Wallace M, Brennan L, Stanton C, Marchesi JR, Fitzgerald AP, Shanahan F, Hill C, Ross RP, O'Toole PW. 2012. Gut microbiota composition correlates with diet and health in the elderly. Nature 488:178–184. https://doi.org/10.1038/nature11319.
6. Garrett WS, Gordon JI, Glimcher LH. 2010. Homeostasis and inflammation in the intestine. Cell 140:859–870. https://doi.org/10.1016/j.cell.2010.01.023.
7. Costello EK, Lauber CL, Hamady M, Fierer N, Gordon JI, Knight R. 2009. Bacterial community variation in human body habitats across space and time. Science 326:1694–1697. https://doi.org/10.1126/science.1177486.
8. Qin J, Li R, Raes J, Arumugam M, Burgdorf KS, Manichanh C, Nielsen T, Pons N, Levenez F, Yamada T, Mende DR, Li J, Xu J, Li S, Li D, Cao J, Wang B, Liang H, Zheng H, Xie Y, Tap J, Lepage P, Bertalan M, Batto J-M, Hansen T, Le Paslier D, Linneberg A, Nielsen HB, Pelletier E, Renault P, Sicheritz-Ponten T, Turner K, Zhu H, Yu C, Li S, Jian M, Zhou Y, Li Y, Zhang X, Li S, Qin N, Yang H, Wang J, Brunak S, Dore J, Guarner F, Kristiansen K, Pedersen O, Parkhill J, Weissenbach J, et al. 2010. A human gut microbial gene catalogue established by metagenomic sequencing. Nature 464:59–65. https://doi.org/10.1038/nature08821.
9. Arumugam M, Raes J, Pelletier E, Le Paslier D, Yamada T, Mende DR, Fernandes GR, Tap J, Bruls T, Batto J-M, Bertalan M, Borruel N, Casellas F, Fernandez L, Gautier L, Hansen T, Hattori M, Hayashi T, Kleerebezem M, Kurokawa K, Leclerc M, Levenez F, Manichanh C, Nielsen HB, Nielsen T, Pons N, Poulain J, Qin J, Sicheritz-Ponten T, Tims S, Torrents D, Ugarte E, Zoetendal EG, Wang J, Guarner F, Pedersen O, de Vos WM, Brunak S, Dore J, MetaHIT Consortium, Antolín M, Artiguenave F, Blottiere HM, Almeida M, Brechot C, Cara C, Chervaux C, Cultrone A, Delorme C, Denariaz G, et al. 2011. Enterotypes of the human gut microbiome. Nature 473:174–180. https://doi.org/10.1038/nature09944.
10. Gow NAR, van de Veerdonk FL, Brown AJP, Netea MG. 2012. *Candida albicans* morphogenesis and host defence: discriminating invasion from colonization. Nat Rev Micro 10:112–122. https://doi.org/10.1038/nrmicro2711.
11. Moran C, Grussemeyer CA, Spalding JR, Benjamin DK, Jr, Reed SD. 2009. *Candida albicans* and non-*albicans* bloodstream infections in adult and pediatric patients: comparison of mortality and costs. Pediatr Infect Dis J 28:433–435. https://doi.org/10.1097/INF.0b013e3181920ffd.
12. Huffnagle GB, Noverr MC. 2013. The emerging world of the fungal microbiome. Trends Microbiol 21:334–341. https://doi.org/10.1016/j.tim.2013.04.002.
13. Wisplinghoff H, Ebbers J, Geurtz L, Stefanik D, Major Y, Edmond MB, Wenzel RP, Seifert H. 2014. Nosocomial bloodstream infections due to *Candida* spp. in the USA: species distribution, clinical features and antifungal susceptibilities. Int J Antimicrob Agents 43:78–81. https://doi.org/10.1016/j.ijantimicag.2013.09.005.
14. Kabir MA, Hussain MA, Ahmad Z. 2012. *Candida albicans*: a model organism for studying fungal pathogens. ISRN Microbiol 2012:538694. https://doi.org/10.5402/2012/538694.
15. Wenzel RP, Edmond MB. 2001. The impact of hospital-acquired bloodstream infections. Emerg Infect Dis 7:174–177. https://doi.org/10.3201/eid0702.010203.
16. Nguyen MH, Peacock J, James E, Morris AJ, Tanner DC, Nguyen ML, Snydman DR, Wagener MM, Rinaldi MG, Yu VL. 1996. The changing face of candidemia: emergence of non-*Candida albicans* species and antifungal resistance. Am J Med 100:617–623. https://doi.org/10.1016/S0002-9343(95)00010-0.
17. Pfaller MA, Jones RN, Castanheira M. 2014. Regional data analysis of *Candida* non-*albicans* strains collected in United States medical sites over a 6-year period, 2006–2011. Mycoses 57:602–611. https://doi.org/10.1111/myc.12206.
18. Azie N, Neofytos D, Pfaller M, Meier-Kriesche HU, Quan SP, Horn D. 2012. The PATH (Prospective Antifungal Therapy) Alliance registry and invasive fungal infections: update 2012. Diagn Microbiol Infect Dis 73:293–300. https://doi.org/10.1016/j.diagmicrobio.2012.06.012.
19. Okada K, Nakazawa S, Yokoyama A, Kashiwazaki H, Kobayashi K, Yamazaki Y. 2016. A clinical study of *Candida albicans* and *Candida glabrata* co-infection of oral candidiasis. Ronen Shika Igaku 31:346–353. https://doi.org/10.11259/jsg.31.346.
20. Coco BJ, Bagg J, Cross LJ, Jose A, Cross J, Ramage G. 2008. Mixed *Candida albicans* and *Candida glabrata* populations associated with the pathogenesis of denture stomatitis. Oral Microbiol Immunol 23:377–383. https://doi.org/10.1111/j.1399-302X.2008.00439.x.
21. Pfaller MA, Messer SA, Hollis RJ, Jones RN, Diekema DJ. 2002. *In vitro* activities of ravuconazole and voriconazole compared with those of four approved systemic antifungal agents against 6,970 clinical isolates of *Candida* spp. Antimicrob Agents Chemother 46:1723–1727. https://doi.org/10.1128/AAC.46.6.1723-1727.2002.
22. Pfaller MA, Boyken L, Messer SA, Tendolkar S, Hollis RJ, Diekema DJ. 2004. Evaluation of the Etest method using Mueller-Hinton agar with glucose and methylene blue for determining amphotericin B MICs for 4,936 clinical isolates of *Candida* species. J Clin Microbiol 42:4977–4979. https://doi.org/10.1128/JCM.42.11.4977-4979.2004.
23. Davies A, Brailsford S, Broadley K, Beighton D. 2002. Oral yeast carriage in patients with advanced cancer. Oral Microbiol Immunol 17:79–84. https://doi.org/10.1046/j.0902-0055.2001.00095.x.
24. Kuhn DM, George T, Chandra J, Mukherjee PK, Ghannoum MA. 2002. Antifungal susceptibility of *Candida* biofilms: unique efficacy of amphotericin B lipid formulations and echinocandins. Antimicrob Agents Chemother 46:1773–1780. https://doi.org/10.1128/AAC.46.6.1773-1780.2002.
25. Silva S, Negri M, Henriques M, Oliveira R, Williams DW, Azeredo J. 2011. Adherence and biofilm formation of non-*Candida albicans Candida* species. Trends Microbiol 19:241–247. https://doi.org/10.1016/j.tim.2011.02.003.
26. Hawser SP, Douglas LJ. 1995. Resistance of *Candida albicans* biofilms to antifungal agents *in vitro*. Antimicrob Agents Chemother 39:2128–2131. https://doi.org/10.1128/AAC.39.9.2128.
27. Uppuluri P, Chaturvedi AK, Srinivasan A, Banerjee M, Ramasubramaniam AK, Kohler JR, Kadosh D, Lopez-Ribot JL. 2010. Dispersion as an important step in the *Candida albicans* biofilm developmental cycle. PLoS Pathog 6:e1000828. https://doi.org/10.1371/journal.ppat.1000828.
28. Chandra J, Kuhn DM, Mukherjee PK, Hoyer LL, McCormick T, Ghannoum MA. 2001. Biofilm formation by the fungal pathogen *Candida albicans*: development, architecture, and drug resistance. J Bacteriol 183:5385–5394. https://doi.org/10.1128/JB.183.18.5385-5394.2001.
29. Tati S, Davidow P, McCall A, Hwang-Wong E, Rojas IG, Cormack B, Edgerton M. 2016. *Candida glabrata* binding to *Candida albicans* hyphae enables its development in oropharyngeal candidiasis. PLoS Pathog 12:e1005522. https://doi.org/10.1371/journal.ppat.1005522.
30. Harriott MM, Noverr MC. 2009. *Candida albicans* and *Staphylococcus aureus* form polymicrobial biofilms: effects on antimicrobial resistance. Antimicrob Agents Chemother 53:3914–3922. https://doi.org/10.1128/AAC.00657-09.
31. Pathak AK, Sharma S, Shrivastva P. 2012. Multi-species biofilm of *Candida albicans* and non-*Candida albicans Candida* species on acrylic substrate. J Appl Oral Sci 20:70–75. https://doi.org/10.1590/S1678-77572012000100013.
32. Heisel T, Montassier E, Johnson A, Al-Ghalith G, Lin Y-W, Wei L-N, Knights D, Gale CA. 2017. High-fat diet changes fungal microbiomes and interk-

ingdom relationships in the murine gut. mSphere 2:e00351-17. https://doi.org/10.1128/mSphere.00351-17.
33. Calderone RA, Fonzi WA. 2001. Virulence factors of *Candida albicans*. Trends Microbiol 9:327–335. https://doi.org/10.1016/S0966-842X(01)02094-7.
34. Sudbery PE. 2011. Growth of *Candida albicans* hyphae. Nat Rev Microbiol 9:737–748. https://doi.org/10.1038/nrmicro2636.
35. Iraqui I, Garcia-Sanchez S, Aubert S, Dromer F, Ghigo J-M, D'Enfert C, Janbon G. 2005. The Yak1p kinase controls expression of adhesins and biofilm formation in *Candida glabrata* in a Sir4p-dependent pathway. Mol Microbiol 55:1259–1271. https://doi.org/10.1111/j.1365-2958.2004.04475.x.
36. Barros PP, Ribeiro FC, Rossoni RD, Junqueira JC, Jorge AO. 2016. Influence of *Candida krusei* and *Candida glabrata* on *Candida albicans* gene expression in *in vitro* biofilms. Arch Oral Biol 64:92–101. https://doi.org/10.1016/j.archoralbio.2016.01.005.
37. Nobile CJ, Nett JE, Andes DR, Mitchell AP. 2006. Function of *Candida albicans* adhesin Hwp1 in biofilm formation. Eukaryot Cell 5:1604–1610. https://doi.org/10.1128/EC.00194-06.
38. Joo MY, Shin JH, Jang HC, Song ES, Kee SJ, Shin MG, Suh SP, Ryang DW. 2013. Expression of SAP5 and SAP9 in *Candida albicans* biofilms: comparison of bloodstream isolates with isolates from other sources. Med Mycol 51:892–896. https://doi.org/10.3109/13693786.2013.824623.
39. Naglik JR, Moyes D, Makwana J, Kanzaria P, Tsichlaki E, Weindl G, Tappuni AR, Rodgers CA, Woodman AJ, Challacombe SJ, Schaller M, Hube B. 2008. Quantitative expression of the *Candida albicans* secreted aspartyl proteinase gene family in human oral and vaginal candidiasis. Microbiology 154:3266–3280. https://doi.org/10.1099/mic.0.2008/022293-0.
40. Vale-Silva LA, Moeckli B, Torelli R, Posteraro B, Sanguinetti M, Sanglard D. 2016. Upregulation of the adhesin gene EPA1 mediated by PDR1 in *Candida glabrata* leads to enhanced host colonization. mSphere 1:e00065-15. https://doi.org/10.1128/mSphere.00065-15.
41. Lamfon H, Porter SR, McCullough M, Pratten J. 2004. Susceptibility of *Candida albicans* biofilms grown in a constant depth film fermentor to chlorhexidine, fluconazole and miconazole: a longitudinal study. J Antimicrob Chemother 53:383–385. https://doi.org/10.1093/jac/dkh071.
42. Mukherjee PK, Chandra J, Retuerto M, Sikaroodi M, Brown RE, Jurevic R, Salata RA, Lederman MM, Gillevet PM, Ghannoum MA. 2014. Oral mycobiome analysis of HIV-infected patients: identification of *Pichia* as an antagonist of opportunistic fungi. PLoS Pathog 10:e1003996. https://doi.org/10.1371/journal.ppat.1003996.
43. Kim D, Sengupta A, Niepa TH, Lee BH, Weljie A, Freitas-Blanco VS, Murata RM, Stebe KJ, Lee D, Koo H. 2017. *Candida albicans* stimulates *Streptococcus mutans* microcolony development via cross-kingdom biofilm-derived metabolites. Sci Rep 7:41332. https://doi.org/10.1038/srep41332.
44. van Leeuwen PT, van der Peet JM, Bikker FJ, Hoogenkamp MA, Oliveira Paiva AM, Kostidis S, Mayboroda OA, Smits WK, Krom BP. 2016. Interspecies interactions between *Clostridium difficile* and *Candida albicans*. mSphere 1:e00187-16. https://doi.org/10.1128/mSphere.00187-16.
45. Redding SW, Dahiya MC, Kirkpatrick WR, Coco BJ, Patterson TF, Fothergill AW, Rinaldi MG, Thomas CR, Jr. 2004. *Candida glabrata* is an emerging cause of oropharyngeal candidiasis in patients receiving radiation for head and neck cancer. Oral Surg Oral Med Oral Pathol Oral Radiol Endod 97:47–52. https://doi.org/10.1016/j.tripleo.2003.09.008.
46. Rocco TR, Reinert SE, Simms HH. 2000. Effects of fluconazole administration in critically ill patients: analysis of bacterial and fungal resistance. Arch Surg 135:160–165. https://doi.org/10.1001/archsurg.135.2.160.
47. Lortholary O, Desnos-Ollivier M, Sitbon K, Fontanet A, Bretagne S, Dromer F, Grp FMS. 2011. Recent exposure to caspofungin or fluconazole influences the epidemiology of candidemia: a prospective multicenter study involving 2,441 patients. Antimicrob Agents Chemother 55:532–538. https://doi.org/10.1128/AAC.01128-10.
48. Guleri A, Gatt D, Sharma R, Pettit S. 2013. Treatment of *Candida glabrata* with micafungin: a case report and brief review of the literature. J Med Cases 4:393–397. https://doi.org/10.4021/jmc1237w.
49. Chong PP, Lee YL, Tan BC, Ng KP. 2003. Genetic relatedness of *Candida* strains isolated from women with vaginal candidiasis in Malaysia. J Med Microbiol 52:657–666. https://doi.org/10.1099/jmm.0.04973-0.
50. Rajendran R, Sherry L, Nile CJ, Sherriff A, Johnson EM, Hanson MF, Williams C, Munro CA, Jones BJ, Ramage G. 2016. Biofilm formation is a risk factor for mortality in patients with *Candida albicans* bloodstream infection-Scotland, 2012–2013. Clin Microbiol Infect 22:87–93. https://doi.org/10.1016/j.cmi.2015.09.018.
51. Vazquez JA. 1999. Options for the management of mucosal candidiasis in patients with AIDS and HIV infection. Pharmacotherapy 19:76–87. https://doi.org/10.1592/phco.19.1.76.30509.
52. Fidel J, Paul L, Vazquez JA, Sobel JD. 1999. *Candida glabrata*: review of epidemiology, pathogenesis, and clinical disease with comparison to *C. albicans*. Clin Microbiol Rev 12:80–96.
53. Redding SW, Kirkpatrick WR, Dib O, Fothergill AW, Rinaldi MG, Patterson TF. 2000. The epidemiology of non-*albicans Candida* in oropharyngeal candidiasis in HIV patients. Spec Care Dentist 20:178–181. https://doi.org/10.1111/j.1754-4505.2000.tb00015.x.
54. Kucharíková S, Tournu H, Lagrou K, Van Dijck P, Bujdakova H. 2011. Detailed comparison of *Candida albicans* and *Candida glabrata* biofilms under different conditions and their susceptibility to caspofungin and anidulafungin. J Med Microbiol 60:1261–1269. https://doi.org/10.1099/jmm.0.032037-0.
55. Monteiro DR, Feresin LP, Arias LS, Barao VA, Barbosa DB, Delbem AC. 2015. Effect of tyrosol on adhesion of *Candida albicans* and *Candida glabrata* to acrylic surfaces. Med Mycol 53:656–665. https://doi.org/10.1093/mmy/myv052.
56. Monteiro DR, Silva S, Negri M, Gorup LF, de Camargo ER, Oliveira R, Barbosa DB, Henriques M. 2013. Antifungal activity of silver nanoparticles in combination with nystatin and chlorhexidine digluconate against *Candida albicans* and *Candida glabrata* biofilms. Mycoses 56:672–680. https://doi.org/10.1111/myc.12093.
57. Hawser SP, Douglas LJ. 1994. Biofilm formation by *Candida* species on the surface of catheter materials *in vitro*. Infect Immun 62:915–921.
58. Cataldi V, Di Campli E, Fazii P, Traini T, Cellini L, Di Giulio M. 2017. *Candida* species isolated from different body sites and their antifungal susceptibility pattern: cross-analysis of *Candida albicans* and *Candida glabrata* biofilms. Med Mycol 55:624–634. https://doi.org/10.1093/mmy/myw126.
59. Pierce CG, Vila T, Romo JA, Montelongo-Jauregui D, Wall G, Ramasubramanian A, Lopez-Ribot JL. 2017. The *Candida albicans* biofilm matrix: composition, structure and function. J Fungi (Basel) 3:14. https://doi.org/10.3390/jof3010014.
60. Alonso MF, Gow NAR, Erwig LP, Bain JM. 2017. Macrophage migration is impaired within *Candida albicans* biofilms. J Fungi (Basel) 3:E31. https://doi.org/10.3390/jof3030031.
61. Kuhn DM. 2002. Comparison of biofilms formed by *Candida albicans* and *Candida parapsilosis* on bioprosthetic surfaces. Infect Immun 70:878–888. https://doi.org/10.1128/IAI.70.2.878-888.2002.
62. Almeida RS, Brunke S, Albrecht A, Thewes S, Laue M, Edwards JE, Filler SG, Hube B. 2008. The hyphal-associated adhesin and invasin Als3 of *Candida albicans* mediates iron acquisition from host ferritin. PLoS Pathog 4:e1000217. https://doi.org/10.1371/journal.ppat.1000217.
63. Sharkey LL, Liao W-L, Ghosh AK, Fonzi WA. 2005. Flanking direct repeats of hisG alter URA3 marker expression at the HWP1 locus of *Candida albicans*. Microbiology 151:1061–1071. https://doi.org/10.1099/mic.0.27487-0.
64. Nailis H, Vandenbroucke R, Tilleman K, Deforce D, Nelis H, Coenye T. 2009. Monitoring ALS1 and ALS3 gene expression during *in vitro Candida albicans* biofilm formation under continuous flow conditions. Mycopathologia 167:9–17. https://doi.org/10.1007/s11046-008-9148-6.
65. Halliwell SC, Smith MCA, Muston P, Holland SL, Avery SV. 2012. Heterogeneous expression of the virulence-related adhesin Epa1 between individual cells and strains of the pathogen *Candida glabrata*. Eukaryot Cell 11:141–150. https://doi.org/10.1128/EC.05232-11.
66. Mundy RD, Cormack B. 2009. Expression of *Candida glabrata* adhesins following exposure to chemical preservatives. J Infect Dis 199:1891–1898. https://doi.org/10.1086/599120.
67. Domergue R, Castaño I, De Las Peñas A, Zupancic M, Lockatell V, Hebel JR, Johnson D, Cormack BP. 2005. Nicotinic acid limitation regulates silencing of *Candida* adhesins during UTI. Science 308:866. https://doi.org/10.1126/science.1108640.
68. Huang M, McClellan M, Berman J, Kao KC. 2011. Evolutionary dynamics of *Candida albicans* during *in vitro* evolution. Eukaryot Cell 10:1413–1421. https://doi.org/10.1128/EC.05168-11.
69. Peeters E, Nelis HJ, Coenye T. 2008. Comparison of multiple methods for quantification of microbial biofilms grown in microtiter plates. J Microbiol Methods 72:157–165. https://doi.org/10.1016/j.mimet.2007.11.010.
70. Schneider CA, Rasband WS, Eliceiri KW. 2012. NIH Image to ImageJ: 25 years of image analysis. Nat Methods 9:671–675. https://doi.org/10.1038/nmeth.2089.
71. Heydorn A, Nielsen AT, Hentzer M, Sternberg C, Givskov M, Ersboll BK,

Molin S. 2000. Quantification of biofilm structures by the novel computer program COMSTAT. Microbiology 146(Pt 10):2395–2407. https://doi.org/10.1099/00221287-146-10-2395.
72. Vorregaard M. 2008. Comstat2—a modern 3D image analysis environment for biofilms. Informatics and Mathematical Modelling. Master's thesis. Technical University of Denmark, Lyngby, Denmark.
73. CLSI. 2002. Reference method for broth dilution antifungal susceptibility testing of yeasts; approved standard, 2nd ed. M27-A2. CLSI, Wayne, PA.
74. Pierce CG, Uppuluri P, Tristan AR, Wormley FL, Jr, Mowat E, Ramage G, Lopez-Ribot JL. 2008. A simple and reproducible 96-well plate-based method for the formation of fungal biofilms and its application to antifungal susceptibility testing. Nat Protoc 3:1494–1500. https://doi.org/10.1038/nprot.2008.141.
75. Chandra J, Mukherjee PK, Ghannoum MA. 2008. *In vitro* growth and analysis of *Candida* biofilms. Nat Protoc 3:1909–1924. https://doi.org/10.1038/nprot.2008.192.